

Isoscalar giant resonances in ^{208}Pb —in particular $2\hbar\omega$ $L=0, 2, 4,$ and 6 excitations—studied in small angle α scattering

H. P. Morsch, P. Decowski,* M. Rogge, P. Turek, L. Zemřo,† S. A. Martin, G. P. A. Berg, W. Hürlimann, J. Meissburger, and J. G. M. Römer

Institut für Kernphysik der Kernforschungsanlage Jülich, D-5170 Jülich, Federal Republic of Germany

(Received 25 January 1983)

Inelastic excitation of giant resonances has been studied in 172 MeV α scattering from ^{208}Pb at scattering angles of 1.5° – 8° . Fine structures in the region of the giant monopole and quadrupole resonances indicate multiplicities also different from $L=0$ and 2. The isoscalar $L=0$ and 2 strengths in the giant resonance region yield $(90\pm 20)\%$ and $(70\pm 20)\%$ of the corresponding energy weighted sum rule limit. This is consistent with other hadron scattering results, with higher energy electron scattering, and with microscopic random phase approximation results. However, the strength for $L=2$ excitations is significantly larger than extracted from lower energy electron scattering. Fine structures observed are compared with high resolution (p,p') and (e,e') results. At scattering angles 5° – 8° new structures have been observed at $E_x=12.5$ and 16.0 MeV consistent with multiplicities $L=4$ and 6. Together with the contribution of higher multipolarity extracted at lower excitation energies from the angular distributions of giant monopole and quadrupole excitations, this indicates rather broad distributions of $2\hbar\omega$ $L=4$ and 6 excitations with centroid energies of 12.2 and 13.7 MeV and widths of 4.5 and 7.8 MeV, respectively. The extracted sum rule strengths for $L=4$ and 6 are in the order of 30% in each case. In the region of the giant monopole resonance evidence for additional $L=2$ excitation was found ($\leq 14\%$ energy weighted sum rule strength). The fact that strong contributions of $L>0$ are obtained solves the problem of a former too large monopole cross section in α scattering which was inconsistent with microscopic descriptions. A recently suggested "antiscaling" mode for the giant monopole resonance, in which the nuclear surface vibrates opposite in phase to the "scaling" mode, can be ruled out by our experimental data. The existence of two odd parity giant resonances at $E_x=18.7$ MeV ($L=3$) and 21.3 MeV ($L=1$) with widths of 5.0 and 5.9 MeV, respectively, are confirmed by our small angle scattering experiments. Our description of the dipole compressional mode is in excellent agreement with 200 MeV proton scattering data.

NUCLEAR REACTIONS $^{208}\text{Pb}(\alpha, \alpha')$; $E_\alpha=172$ MeV. Small angle scattering, $\theta=1.5^\circ$ – 8° ; measured $\sigma(\theta)$. Deduced excitation strength distributions for giant resonances of multiplicities $L=0$ – 6 .

I. INTRODUCTION

There are several open problems concerning giant resonances in ^{208}Pb which are of current interest. Recently, high lying isoscalar giant resonances ($L=3$ and 1) were found in inelastic hadron scattering.^{1–4} Old electron scattering results⁵ are confirmed by the observation of a high lying giant octupole resonance (GOR); the isoscalar $L=1$ excitation ("squeezing mode")^{1,4} represents a new compressional mode of excitation which should be confirmed in other experiments.

Further, there are conflicting reports on the isoscalar $L=2$ strength in the region of the giant quadrupole resonance (GQR). In hadron scattering generally a strong bump is observed at ~ 10.9 MeV (Refs. 1–4 and 6–8) from which an isoscalar $L=2$ strength of $(60$ – $100)\%$ of the energy weighted sum rule (EWSR) limit has been extracted. This is very different from lower energy electron scattering results⁹ in which no strong collective quadrupole strength has been found in this excitation region. In hadron scattering there is evidence for higher multipolari-

ty in the region of the GQR.^{4,8} Because of this the discrepancy between hadron and electron scattering could be resolved if the dominant strength observed in hadron scattering would be due to excitation of higher multiplicities which are only weakly excited in (e,e'). This, however, would mean that one has to give up the concept of a concentrated GQR which is consistent with theory.¹⁰ Related to this problem is the observation of fine structures in the giant quadrupole region which are different in (e,e') (Ref. 11) and (p,p') (Ref. 12) experiments.

Another problem exists in the excitation of the giant monopole resonance (GMR) in α scattering. In a microscopic approach using folding techniques the absolute α scattering cross sections were underpredicted roughly by a factor of 2.^{8,13} Only by assuming strong surface effects (surface compression mode) α scattering data could be fitted.⁸ However, the use of such a transition density is inconsistent with microscopic as well as macroscopic models.^{10,14,15}

To study these questions we performed small angle α scattering experiments in the angular range 1.5° – 8° .

There are two regions of particular interest, the very small angle region $\theta \lesssim 4^\circ$ and the larger angle region $5^\circ \lesssim \theta \lesssim 8^\circ$. In the very small angle region $\theta \lesssim 4^\circ$ the strength of the $L=2$ component in the GQR region can be extracted rather unambiguously because higher multiplicities contribute only weakly. For the correct extraction of the $L=2$ strength the situation in α scattering is quite favorable from the point of view of nuclear dynamics¹⁶: the GQR excitation can be studied at the $L=2$ form factor maximum ($q \sim 0.6 \text{ fm}^{-1}$), leading to strong collective excitation. This is quite different for lower energy electron scattering⁹ in which the GQR excitation is studied only at small momentum transfer ($q \sim 0.25 \text{ fm}^{-1}$) resulting in a rather weak excitation which is difficult to extract from the large electron scattering background. In the angular region 3° – 4° the GOR can be studied (see also Ref. 17). On the other hand, at larger angles of 5° – 8° one can study very nicely higher multipole excitations. The differential cross sections show very distinct differences between excitations of different L value. This allows us to determine the L value of an excitation unambiguously. Since the dominant $L=0, 2,$ and 3 excitations have diffraction minima in this region the yield of higher multiplicities is comparatively large. Further, at about 6° we expect a rather strong excitation of the isoscalar dipole resonance. This allows us to study this interesting compressional mode of excitation in more detail.

II. EXPERIMENTS AND DATA ANALYSIS

The experiments were performed using a 172 MeV α beam from the Jülich isochronous cyclotron JULIC. The emittance of the beam was confined to a few mm mrad using axial phase slits in the cyclotron center and slits in the extraction path specially mounted for small angle experiments. Additional slits in the beam line system were used to clean up the beam. The scattered α particles were momentum analyzed using the Jülich magnetic spectrometer BIG KARL. To cover an excitation energy range of more than 30 MeV the variable dispersion was set to about 3 cm p/100 Δ p. The positions of inelastically scattered particles were measured in the focal plane with a multiwire proportional chamber¹⁸; a plastic scintillator of 1 cm thickness was used for particle identification and fast timing. Clean ^{208}Pb targets of about 8 mg/cm² thickness were used. For almost all runs contamination of ^{12}C could be avoided but not of H which yielded contributions in the giant resonance region at angles between 6.5° and 8° . At these angles the H contribution was fitted and subtracted in the spectra. Separate runs with Mylar targets were made to check position and width of the contaminant peaks (see also the analysis in Ref. 19). To define the background shape (see below) it is important to have a good knowledge of the higher energy continuum above the giant resonances. Therefore, in addition to the measurements covering up to 33–35 MeV of excitation for several angles we used smaller magnetic fields to measure higher excitation energies up to 40–45 MeV.

Small angle α spectra are shown in Fig. 1. For the analysis of these data in the angular range $\leq 4^\circ$ we have used a continuum background shape which is consistent

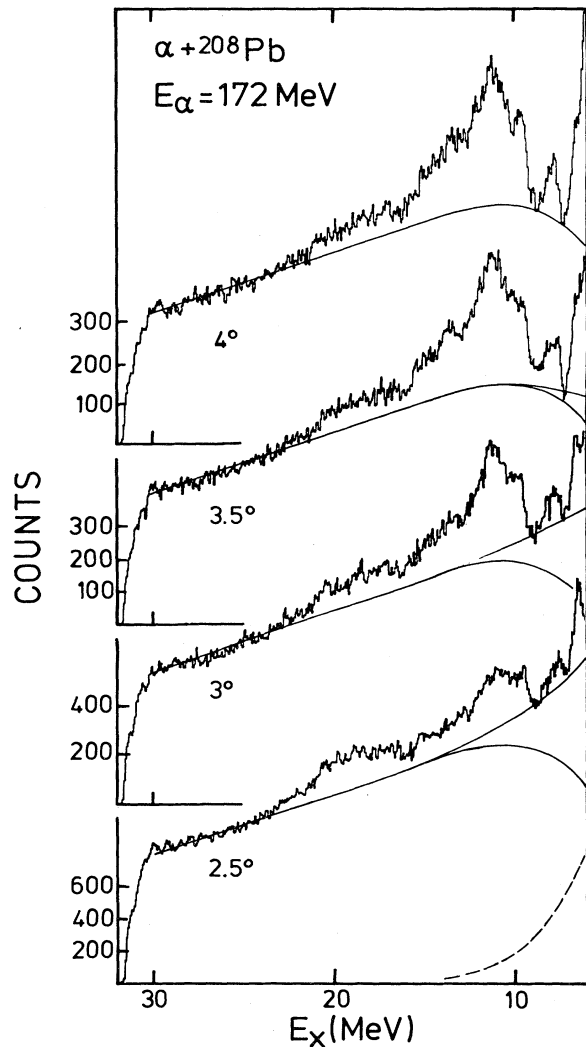


FIG. 1. Small angle α spectra from ^{208}Pb . Consistent background fits are shown using a background distribution fitted at 4° and an additional high energy background due to the tail of the elastic peak fitted at 2° (dashed line).

for all spectra. The spectral shape was determined from the 4° spectrum in the usual way as used in Refs. 1, 17, and 19. This spectral form has been used also for the other spectra applying an appropriate normalization (Fig. 2). Additionally, a second background part was added which originates from the tail of the elastic scattering (high energy background). The shape (dashed line in Fig. 1) was fitted at 2° ; the magnitude scales with the elastic cross section (see Fig. 2). In this way the continuum part of the spectra is well described. The angular behavior of the main background has also an appreciable forward rise indicating a sizable instrumental background at very small angles due to multiple scattered particles. At the smallest angle measured (1.4° – 1.5°) the instrumental background was already rather high and allowed only a rough estimate of GQR and GMR cross section. The high excitation region above ~ 17 MeV could not be studied reliably at an-

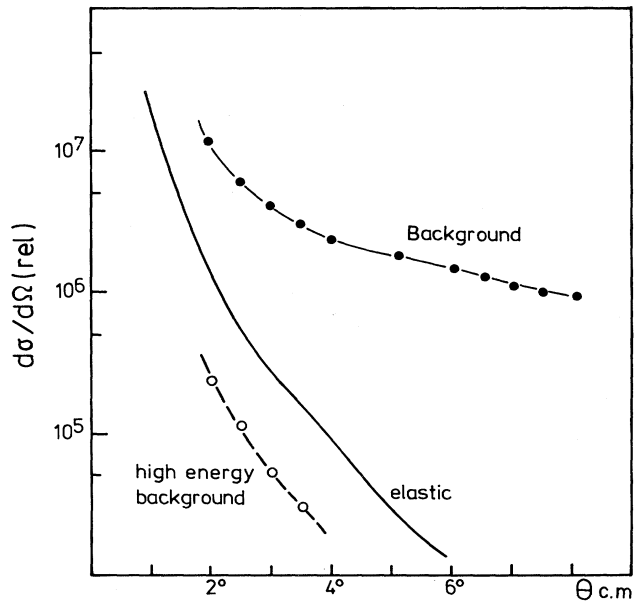


FIG. 2. Angular dependence of the two background contributions in Fig. 1. The solid line indicates the cross section of elastic scattering using the optical potentials from Ref. 8.

gles smaller than 3° due to contributions from scattering on the walls of the vacuum chamber of the spectrometer.

Here, some further remarks on the background subtraction in higher energy hadron scattering should be added. Different from lower energies where more complicated processes like precompound emission contribute to the background in the inelastic scattering, at higher incident energies the inelastic continuum is expected to be dominated by direct excitation (see, e.g., Refs. 20 and 21) which may be interpreted by broad overlapping distributions of many different (mostly higher) multipolarities (see, e.g., Refs. 10 and 22). So we have a situation in which both resonance excitation and continuum are of similar direct character. In this case, rather than to extract cross sections of resonances in an absolute manner in which the full uncertainties of the background subtraction enter, one can determine resonance cross sections for fixed given background shapes. Such cross sections depend, of course, on the background height. Nevertheless, if the background line is drawn sufficiently low the extracted yields should contain the same amount of concentrated (low multipolarity) strength. Different background forms should lead only to extraction of a different amount of the underlying (higher multipole) strength. An example is given in Ref. 1 where the differential cross section of the 13.8 MeV resonance is extracted for two rather different background shapes. Both sets of data^{1,8} with different absolute cross sections yield the same amount of $L=0$ (and $L=1$) strength; the data set derived from the lower background yields additional contributions of higher multipolarity (described by $L=4$ and 6). Therefore, in this approach it is only important to subtract the continuum background in a consistent way for all angles. Uncertainties due to this procedure enter only into the angular dis-

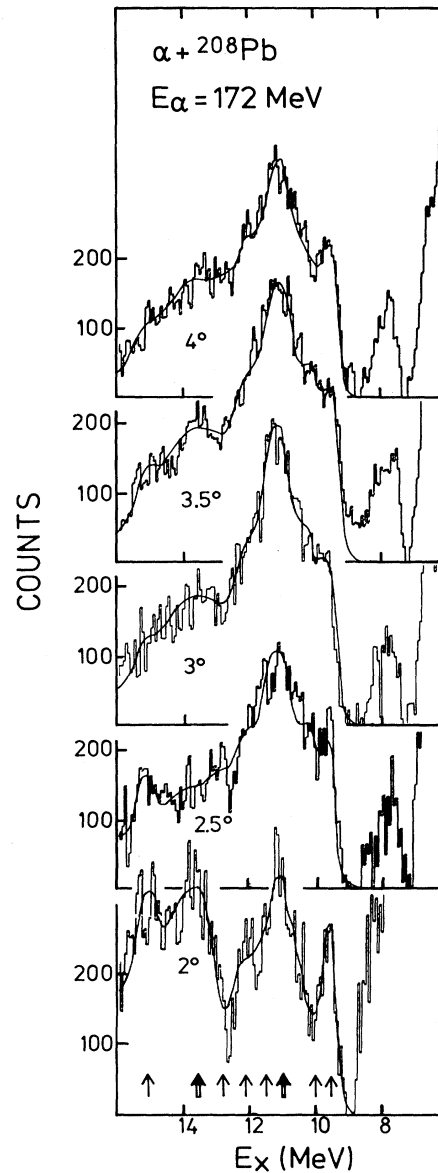


FIG. 3. Giant resonance spectra in the small angle region 2° – 4° after subtraction of the background. The lines indicate a fit to the spectra with peaks given by the arrows on the bottom.

tributions of the extracted resonance peaks. The significance of these peaks can be checked by their appearance at different angles.

Figure 3 shows giant resonance structures in the excitation region 8–16 MeV after subtraction of the continuum background. As observed for larger angles^{1,8} the giant quadrupole excitation at $E_x = 10.9$ MeV is the dominant structure in the spectra. We observe fine structure in the GQR but also in the energy range of the GMR. At angles larger than 3° the spectral form is rather similar to that at larger angles (Ref. 1) whereas at 2° the appearance of giant resonances is very different. This is due to a decrease of the GQR cross section, a rise of the GMR yield, and fine structure peaks which are more pronounced than found at

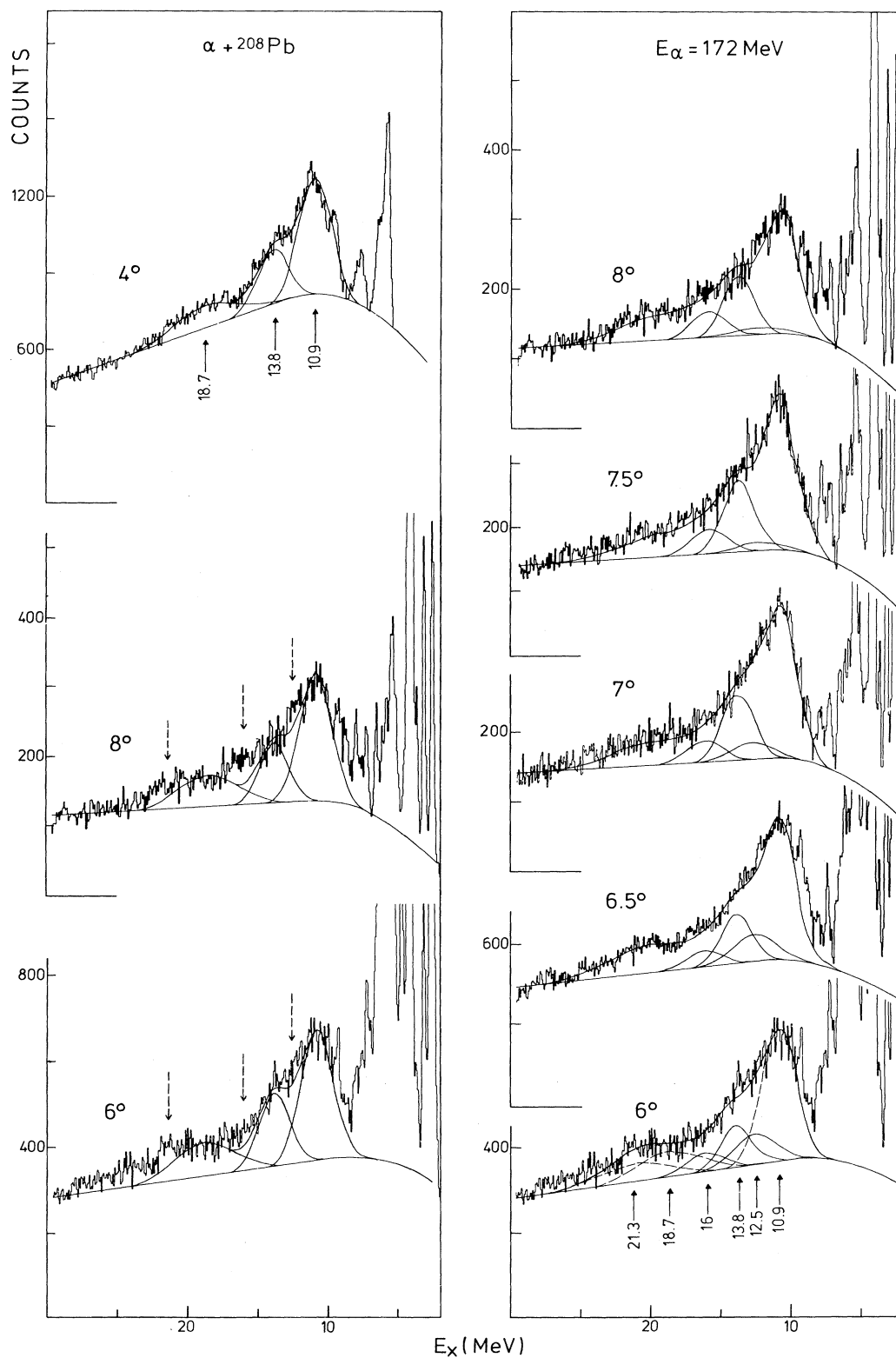


FIG. 4. Comparison of 4° spectrum with the measured spectra at larger angles 6° – 8° . Left-hand side: three Gaussian fits to the giant resonances with the energies indicated. Excitation regions with large deficiencies of the fits are marked by dashed arrows above the 6° and 8° spectra. Right-hand side: fits to the resonances including additional structures at 12.5, 16, and 21.3 MeV. The separate resonances at 12.5, 13.8, and 16 MeV are shown in all spectra.

TABLE I. Resonance parameters and sum rule strengths for $L=0-6$ excitations derived from the data in Figs. 4 and 5 (fit 1). Using only two Gaussian peaks in the region of GQR and GMR the results in Fig. 6 yield sum rule strengths given by fit 2. For these fits the $L=0$ cross section was obtained using a Tassie transition density.

E_x (MeV)	Fit 1 (Fig. 5)			E_x (MeV)	Fit 2 (Fig. 6)		
	Γ (MeV)	L	S (% EWSR)		Γ (MeV)	L	S (% EWSR)
10.9	2.6	2	59	10.9	2.6	2	59
		3	5			3	5
		4	12			4	16
		6	16			6	16
12.5	3.6	4	14				
13.8	2.6	0	90	13.8	2.6	0	90
		1	a			1	a
		2	14			2	14
		6	6			4	9.5
						6	6
16.0	2.9	6	15	16.0	2.9	6	15
18.7	5.0	3	60	18.7	5.0	3	60
21.3	5.9	1	90	21.3	5.9	1	90
						5	5

^aSee Ref. 23.

larger angles. The solid lines in Fig. 3 show an attempt to fit the different spectra with peaks at excitation energies of 9.3, 10.0, 10.9, 11.1, 11.5, 12.2, 12.9, 13.8, and 15.4 MeV with widths [full width at half maximum (FWHM)] of 0.6, 0.6, 2.6, 1.4, 0.6, 0.7, 0.7, 2.6, and 0.7 MeV, respectively. Although the peaks were deduced from all spectra taken between 2° and 4° due to statistical uncertainties the statistical significance of some of the small peaks, e.g., those at 10, 11.5, and 12.9 MeV may be questioned. Fine-structure peaks in the region of the GQR are also seen in the spectra in the $6^\circ-8^\circ$ region (Fig. 4). Here it should be noted that at excitation energies of 10.1, 10.6, and 11.1 MeV pronounced structures have been observed in electron scattering (Refs. 5 and 11). However, these are quite different from the structures in the small angle spectra (Fig. 3). The fits in Fig. 3 indicate rather complex structure with relative yields of the peaks which change differently with angle. This indicates excitations of multipolarity different from the dominant $L=0,2$ excitation in this energy region. As the gross features are still rather well described by two Gaussians (with resonance parameters in Refs. 1 and 8), the small angle data in Figs. 1 and 3 were refitted by two Gaussian peaks at 10.9 and 13.8 MeV widths of 2.6 MeV. These data will be discussed below.

In the angular region $3^\circ-4^\circ$ only the GOR is strongly excited¹⁷ at higher excitation energies (see the discussion below). Because of this the giant resonance bumps can be well approximated in this angular region by three Gaussian peaks which can be identified as GQR, GMR, and GOR (see Fig. 4). Excitation energies and widths for GQR and GMR are taken from Ref. 8 while those for GOR were found to be 18.7 ± 0.7 and 5.0 ± 0.9 MeV, respectively. The location of the GOR is 1 MeV higher than estimated from the analysis of larger angle data¹ and

is in good agreement with p scattering results.²

Going from these small scattering angles to angles of $5^\circ-8^\circ$ a significant change of the giant resonance structure is observed (Fig. 4). There are three regions of energy (indicated by arrows on the left-hand side of Fig. 4) where the simple three Gaussian fit does not give a satisfactory description of the data. These are the regions between GQR and GMR, between GMR and GOR, and above GOR, the latter at the position of the high lying resonance at 21.3 MeV seen in larger angle α scattering.¹

In order to get an improved description of our spectra in the $6^\circ-8^\circ$ region (Fig. 4) we included in our fits in addition to the 21.3 MeV structure¹ resonances at $E_x = 12.5$ and 16 MeV with widths (FWHM) of 3.6 and 2.9 MeV (Table I). These resonances were not apparent in the small angle spectra (Figs. 1 and 3). The yields at 12.5 and 16 MeV are quite different for different angles (peaks indicated on the left side of Fig. 4). Differential cross sections in this angular region are given in Fig. 5; they show rather different features which should enable us to determine the L values. Although details in the region of the GMR and GQR could be well described only by three Gaussian peaks at $E_x = 10.9, 12.5,$ and 13.8 MeV (fits in the right-hand side of Fig. 4, see also Table I, fit 1) a two Gaussian fit for GQR and GMR was performed also (Table I, fit 2) for a direct comparison of the present results with those at larger angles.¹ These results for the GMR are also given in Fig. 5 (open points). The relative differences between two and three Gaussian fits for the GQR are a factor of ~ 3 smaller (therefore cross sections of the 10.9 MeV resonance are not shown in Fig. 5). A comparison of differential cross sections from the small angle experiments with a refit of the larger angle spectra¹ (fit 2) is given in Fig. 6.

To analyze our experimental differential cross sections

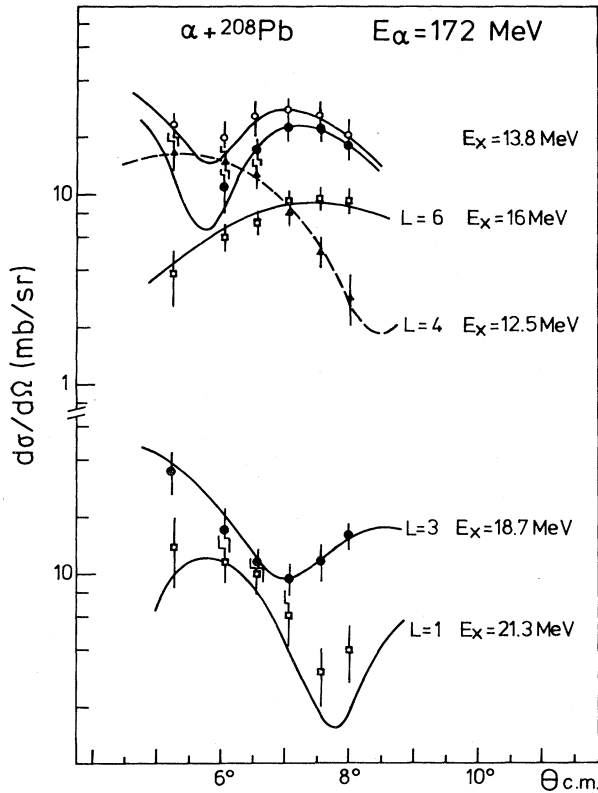


FIG. 5. Differential cross sections for different resonances in the angular region 5° – 8° in comparison with microscopic DWBA calculations discussed in Sec. II. The open points for the 13.8 MeV resonance are obtained from a two Gaussian fit for GMR and GQR (Table I, fit 2).

in Figs. 5 and 6 distorted-wave Born approximation (DWBA) calculations were performed using folding-type form factors. The calculations are similar to those in Refs. 1 and 8 using the same effective nucleon-nucleon interaction, they yield a good description of the data on low lying excitations and giant resonances in Ref. 8. These calculations confirm our experimental finding of a clear L signature in the 5° – 8° region, the structure at 12.5 and 16 MeV could be described only assuming multiplicities $L=4$ and 6 with strengths of 14% and 15% of the corresponding EWSR limit (Fig. 5). This is the first direct evidence for high multipole strength in the giant resonance region of ^{208}Pb . The calculated cross sections for the 13.8 MeV resonance in Fig. 5 are obtained assuming a monopole component (using a Tassie transition density) exhausting 90% of the EWSR strength, excitation of the isovector giant dipole resonance (see Refs. 8 and 23) and additional strength of $L=2$ and 6 with EWSR strengths of 14% and 6% for the lower curve. The higher curve is obtained by adding an $L=4$ component of 9.5% of the EWSR strength. This is the amount of $L=4$ excitation in the 13.8 MeV resonance if the region of the 10.9 and 13.8 MeV resonances is analyzed only by a two Gaussian fit. The small $L=6$ component was taken from Ref. 1; an $L=2$ component in the GMR has recently been report-

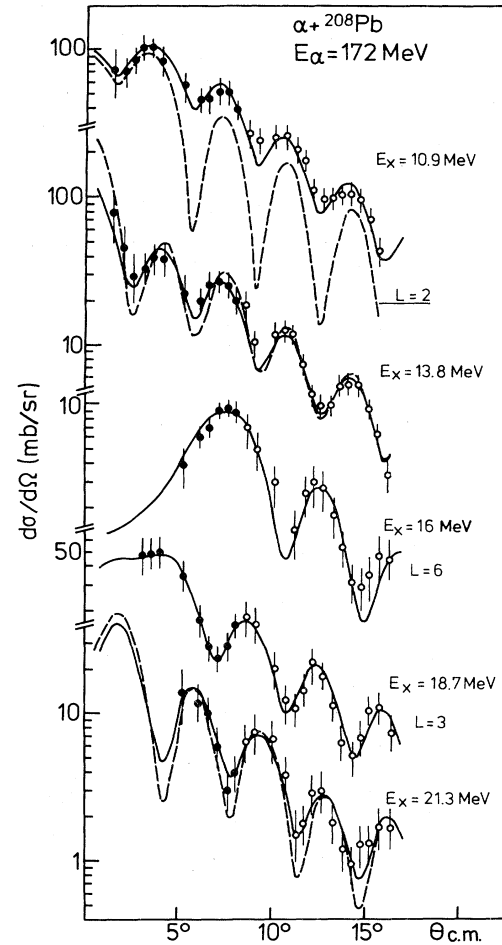


FIG. 6. Differential cross sections for giant resonance excitations from the small angle experiments (solid points) in comparison with larger angle data (open points) from a reanalysis of the spectra in Refs. 1 and 8 using three resonances at higher excitation energies at $E_x = 16$, 18.7, and 21.3 MeV (Table I, fit 2). The solid and dashed lines correspond to microscopic DWBA calculations discussed in the text.

ed.²⁴ The solid lines for the high lying resonances represent calculations assuming $L=3$ and 1 excitations exhausting 60% and 90% of the corresponding EWSR strengths (Fig. 5). The transition density for the isoscalar dipole excitation used was of the form²⁵

$$\rho_{\text{TR}}(r) = j_1(kr) \delta\rho_0 \frac{\partial\rho(r)}{\partial\rho_0} + \delta R \frac{\partial\rho(r)}{\partial R}. \quad (1)$$

The energy weighted sum rule $S(L=1)$ is given by

$$S(L=1) = \frac{33\hbar^2}{8\pi m} A \langle r^4 \rangle \left[1 - \frac{25\langle r^2 \rangle^2}{33\langle r^4 \rangle} \right]. \quad (2)$$

This sum rule differs from that given in Ref. 26 (and used in Ref. 1) by the recoil part $25\langle r^2 \rangle^2/33\langle r^4 \rangle$ which cannot be exhausted by inelastic excitation strength. Therefore, the sum rule (2) (which for ^{208}Pb is smaller than that in Ref. 26 by a factor of 0.41) is more appropriate for a com-

parison with experimental data. In this connection it should be mentioned that also the experimental cross sections for the 21.3 MeV resonance as obtained in the new analysis (Fig. 6) are smaller than those in Ref. 1 by about a factor of 2.

III. DISCUSSION

The spectra in Figs. 1, 3, and 4 indicate a rather complex giant resonance structure. The fact that a new structure was found between GQR and GMR at 12.5 MeV helps to solve the problem of the giant monopole excitation in α scattering. Similarly, the detection of the additional structure at 16 MeV explains the fact that from the larger angle data¹ the GOR was located too low in excitation energy. The inclusion of these new structures in further discussion should give us a more complete and realistic picture of the giant resonance structure of ^{208}Pb . In the following we discuss four subjects: the structure of the giant quadrupole and monopole resonances, the distribution of $2\hbar\omega$ higher multipole strength, and odd parity excitations at higher excitation energies.

A. The region of the GQR at $E_x \sim 10.9$ MeV

Differential cross sections for the excitation of the GQR at $E_x = 10.9$ MeV are shown in Fig. 6 in comparison with DWBA calculations. In contrast to a pure $L=2$ cal-

ulation (dashed line) the angular distribution is rather flat. This was taken as evidence for contributions of higher multipolarity.⁸ In Ref. 8 the excitation of the GQR was studied in two different scattering systems, α and d scattering. A consistent description of both systems yielded strong contributions of higher multipolarity. The solid line shown for $E_x = 10.9$ MeV in Fig. 6 represents the same calculation as published in Ref. 8 (fit 1). It contains EWSR strengths of 59% for $L=2$, 5% for $L=3$, and 16% for each $L=4$ and 6 (Table I). This calculation (obtained from a fit to the larger angle data in α and d scattering²⁷) also yields a good description of the small angle cross sections obtained in the present experiment. The result of a large strength of higher multipolarity ($L=4$ and 6) in the GQR region is nicely confirmed by a $^{208}\text{Pb}(\alpha, \alpha'n)$ correlation experiment.²⁸ The decay into the $\frac{13}{2}^+$ state in ^{207}Pb was found to exhaust about 20% of the total strength in the GQR region; this is consistent with our large $L=6$ (and $L=4$) component.

In the small angle region the differential cross section is dominated by $L=2$ excitation; thus the quadrupole component is quite well determined by the small angle data. The fact that our small angle data are well described indicates a $L=2$ strength of $(60 \pm 10)\%$ of the isoscalar EWSR strength. This is in good agreement with microscopic random phase approximation (RPA) calculations.¹⁰ Our results of a concentrated $L=2$ resonance are also in

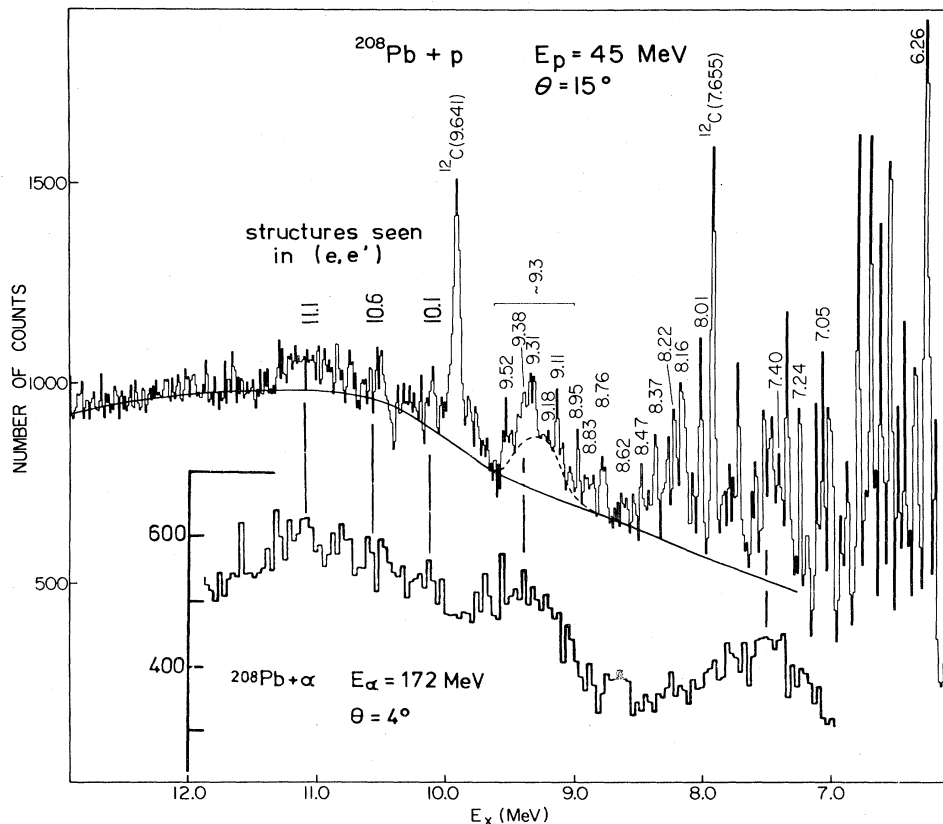


FIG. 7. Comparison of the 4° spectrum with the high resolution (p,p') spectrum of Ref. 12.

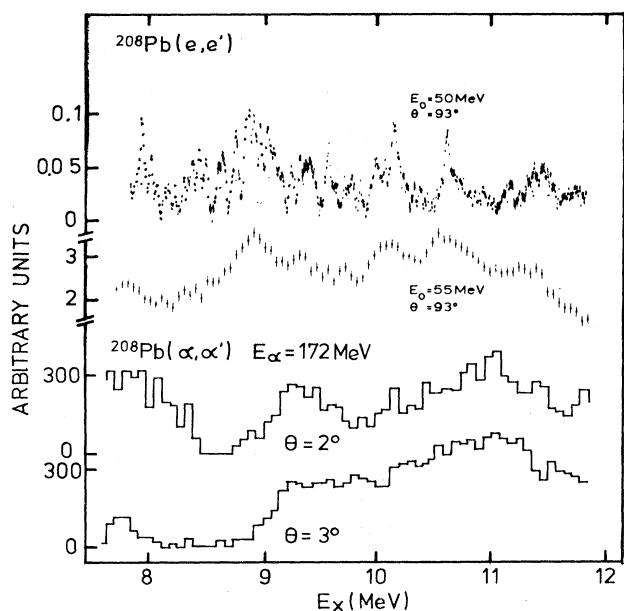


FIG. 8. Comparison of the background subtracted 2° and 3° spectra with the (e,e') spectra in Ref. 9.

good agreement with higher energy electron scattering,⁵ however, they are in strong disagreement with a recent study⁹ of lower energy (e,e') in which only a small $L=2$ strength of about 30% of the EWSR strength has been extracted. Moreover, most of this strength is found in a peak at about 8.9 MeV for which quite controversial interpretations exist in the literature (see Ref. 29). This 8.9 MeV peak is not observed in our α spectra, so it cannot contain a large fraction of the isoscalar $L=2$ strength.

In Figs. 7 and 8 our small angle spectra are compared with high resolution (p,p') (Ref. 12) and (e,e') (Ref. 9) spectra. In the GQR region a rather good correspondence of p and α spectra is observed. The structure at 9.3 MeV which is clearly seen in (p,p') has been interpreted mainly

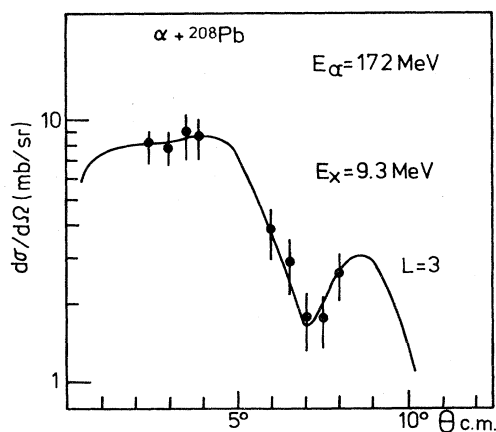


FIG. 9. Differential cross sections for the peak at 9.3 MeV in comparison with a DWBA calculation for $L=3$. A background was assumed similar to that in Ref. 12 (Fig. 7).

as $L=3$ excitation.¹² Cross sections for this peak are shown in Fig. 9. They indicate a multipolarity $L=3$ with an EWSR strength of 5%. It is interesting to note that the same $L=3$ strength has been extracted from a fit of the total GQR cross section⁸ in Fig. 6 (see Table I). Thus this excitation carries the whole $L=3$ strength in this excitation region. The pronounced triple structure (see Fig. 8) with peaks at 10.1, 10.6, and 11.1 MeV seen in (e,e') (Ref. 11) was not strongly seen in the high resolution (p,p') experiment¹² (experimental resolution ~ 20 keV). In several of our α spectra fine-structure peaks have been observed at these energies but with rather small yields. Therefore, these structures cannot be purely $L=2$, a conclusion which is in agreement with a recent (γ,γ) and (γ,n) study³⁰ in which these structures were attributed to dipole excitation.

Different from (p,p') the comparison of our data with the (e,e') spectra⁹ (Fig. 8) shows little similarity. Of course, the strong $L=3$ peak at 9.3 MeV should not be excited at low momentum transfer in (e,e') ; on the other hand, isovector excitations are not observed in α scattering. As indicated above, in the excitation region of the 8.9 MeV state seen in (e,e') (Ref. 9) there is a minimum yield in our α spectra, as well as in p and ^3He spectra.¹² Thus this peak cannot be of dominant isoscalar nature. Compared to the lower energy (e,e') our spectra are in much better agreement with those at higher energy electron scattering.⁵ Quite interestingly, also in a recent (p,p') experiment at $E_p=201$ MeV (Ref. 4) a peak has been observed at $E_x \sim 9$ MeV with a width of 1 MeV. Since 200 MeV proton scattering is also different from an isoscalar probe this may indicate again another type of excitation than isoscalar $L=2$, as claimed in Ref. 4, possibly related to spin flip.

B. The region of the GMR at 13.8 MeV

Differential cross sections for the GMR region are shown in Fig. 6 in comparison with the larger angle data. The yields analyzed by the smooth background form used in Ref. 1 and also in the present analysis contain contributions of L values which were fitted by 3.5% $L=4$ and 6% $L=6$ EWSR strength.¹ These multipole components were also assumed in our present analysis. Remarkably, our detailed analysis of the $6^\circ-8^\circ$ spectra revealed a much larger concentration of $L=4$ strength at 12.5 MeV with a sum rule strength of 14% (Fig. 5 and Table I, fit 1). This indicates that the GMR cross section is definitely smaller than extracted from the larger angle measurements,⁸ at 6° it is not more than 60% of the total cross section of the 13.8 MeV resonance. This solves the problem of too large monopole cross sections in α scattering⁸ which could be reproduced only by assuming a dominant monopole surface vibration (dashed line in Fig. 6, the details of this calculation are the same as discussed in Refs. 1 and 8).

A good description of our data can be obtained in different ways. Assuming a monopole transition from the scaling model (Tassie transition density) the absolute cross sections are obtained by assuming an additional $L=2$ component of 14% EWSR strength (Table I). This is shown by the solid lines in Figs. 5 and 6 which yield a

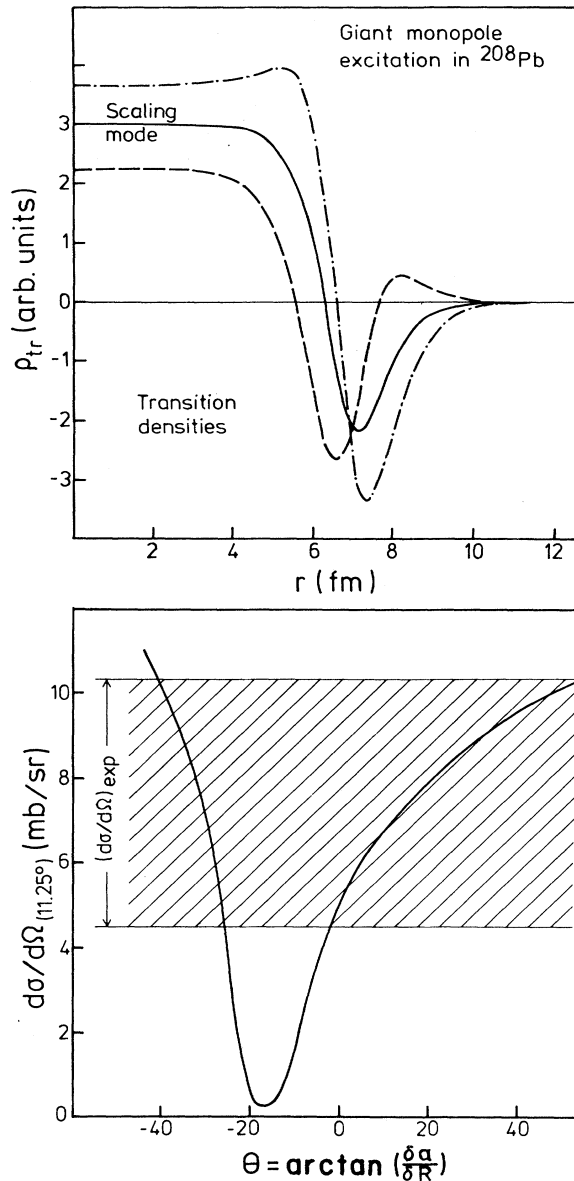


FIG. 10. Monopole transition densities and calculated (α, α') cross sections for the GMR excitation as a function of the relative amount of surface contribution using transition densities of the form of $\rho_{\text{TR}3}$ in Ref. 8. In the upper part the solid, dot-dashed, and dashed lines indicate transition densities (see text) with $\theta=4^\circ$, 30° , and -20° , respectively. The hatched area in the lower part indicates the experimental $L=0$ cross sections which have larger uncertainties due to $L=2$ ambiguities (see Sec. III B).

good description of the 13.8 MeV data. A $L=2$ component at this energy would indicate a high energy tail of the GQR consistent with theoretical predictions.^{10,22,31} The assumption of a $L=2$ component is also consistent with a recent study of small angle α scattering at lower incident energy.²⁴ Almost equally good descriptions of our data can be obtained assuming larger $L=0$ cross sections up to a factor of 1.5 and correspondingly smaller $L=2$

yields. Larger $L=0$ cross sections are obtained if stronger surface effects are assumed. The dependence of the α scattering cross section on the amount of surface vibration is shown in Fig. 10 assuming transition densities of the form of $\rho_{\text{TR}3}$ in Ref. 8. Here θ is related to the surface amplitude δa by $\theta = \arctan(\delta a / \delta R)$ (see the discussion of surface effects in Ref. 32). In Fig. 10 also the experimental limits on the monopole cross sections are given by the hatched area. Owing to the ambiguities between $L=0$ and 2 yields the exact amount of surface contribution cannot be obtained from our data. More detailed information can be obtained only at 0° where larger differences exist between the dashed and the solid lines in Fig. 6. Nevertheless, a monopole vibration of “antiscaling” type which was recently suggested from static calculations³³ can be ruled out by our experiment. In such a mode of vibration ($\theta \sim -10^\circ$ to -20°) in which the surface oscillates opposite in phase to the scaling mode, α scattering cross sections are obtained which are a factor of 5 smaller than those obtained from a pure volume vibration ($\theta=0^\circ$) which can be considered as lower limit of the experimental monopole cross sections (Fig. 10). In Fig. 10 monopole transition densities are also shown which correspond to different vibration modes, scaling mode ($\theta=4^\circ$), stronger surface vibration ($\theta=30^\circ$), and “antiscaling” mode ($\theta=-20^\circ$).

C. The distribution of $2\hbar\omega$ $L=2, 4,$ and 6 excitation strengths

The structures found at excitation energies of 12.5 and 16 MeV indicate higher multipole strength in the $2\hbar\omega$ excitation region of ^{208}Pb predicted by RPA calculations.¹⁰ The shapes of the differential cross sections in the 5° – 8° region can be described only by adding contributions of multiplicities $L=4$ ($E_x=12.5$ MeV) and $L=6$ ($E_x=16$ MeV). The fact that these structures were not seen at small angles supports the assumption of higher multiplicities. The high excitation region in the larger angle data¹ which was analyzed by two resonances (at $E_x=17.5$ and 21.3 MeV) has been reanalyzed using three resonances at 16, 18.7, and 21.3 MeV. The 16 MeV cross sections in Fig. 6 are consistent with the small angle data described by $L=6$ (Table I). The fact that for $\theta \geq 8^\circ$ the $L=6$ and 3 angular distributions are in phase (Fig. 6) explains why in the previous study¹ only two resonances were extracted, the GOR at too low an excitation energy. The information on multipole strengths from the excitations at 12.5 and 16 MeV can be combined with the analysis of the GQR and GMR cross sections in Fig. 6 from which also higher multipole strength has been derived (Table I). In the region of the GQR the $L=4$ and 6 multipole strength has an energy distribution quite similar to that of $L=2$: Studying the spectra at the $L=2$ diffraction maxima and minima the $L=2$ yield (dashed line in Fig. 6) is different by 1 order of magnitude. Nevertheless, the spectral shape of the experimental GQR bump is hardly affected. This indicates quite similar shapes for the different multipole components $L=2, 4,$ and 6 . Differences are observed for the fine-structure peaks which are seen more clearly for some angles but not for others. This indicates that they

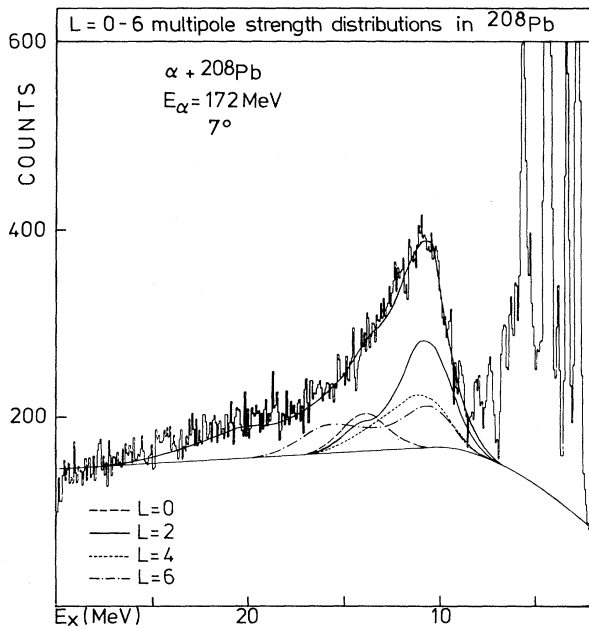


FIG. 11. Relative multipole strengths distributions for even multiplicities obtained from our analysis of the resonances at 10.9, 12.5, 13.8, and 16 MeV.

are related to certain multiplicities $L \neq 2$. This is confirmed by the $^{208}\text{Pb}(\alpha, \alpha'n)$ experiment²⁸ in which these structures were found to be different in different decay channels.

In Fig. 11 the different L components from the peaks at 10.9, 12.5, 13.8, and 16 MeV (Fig. 1, Table I) are summed up separately. Uncertainties in the relative strength distribution for $L=2$ exist in the GMR region where the extracted $L=2$ excitation depends on the monopole cross section (discussed in Sec. III B). In Fig. 11 the $L=2$ component is taken from the fit given by the solid lines in Figs. 5 and 6 (using of Tassie transition density for $L=0$). Furthermore, larger uncertainties in the high energy tails of the multipole distributions are due to the used Gaussian resonance shapes and the subtracted continuum background yield. The distributions in Fig. 11 are quite different from Gaussian shapes. Centroid energies of 11.4 MeV for $L=2$, 12.2 MeV for $L=4$, and 13.7 MeV for $L=6$ were extracted with widths (FWHM) of about 2.7, 4.5, and 7.8 MeV, respectively. The total multipole strength extracted from the different resonances (Table I) is about 70% for $L=2$, 90% for $L=0$, and 30% for both $L=4$ and 6. The uncertainties of these numbers due to background and fits are estimated to be $\pm 20\%$ for $L=0$ and 2 and $\pm 10\%$ for $L=4$ and 6. Of course, all these estimates are based on the background form subtracted (discussed in Sec. II). Assuming an even lower background we cannot exclude additional less concentrated strength of higher multiplicities ($L=4, 6$, and possibly even $L=8$ in the $2\hbar\omega$ region).

The multipole strength distributions in Fig. 11 can be well understood in a schematic picture: By the effective particle-hole interaction which is strongly attractive for

$L=2$ the quadrupole centroid energy is pushed down from the unperturbed $2\hbar\omega$ excitation (~ 14 MeV in ^{208}Pb) by about 3 MeV. For higher multipolarity the effective force is weaker, for $L=6$ it is already very weak and does not lead to a shift of centroid energy. On the other hand, the width of the multipole distribution increases for increasing multipolarity. This picture is nicely supported by microscopic calculations.^{10,22}

D. High lying odd parity giant resonances

From differences in the spectral form at different angles (see Fig. 4) it is quite obvious that the high excitation region exists of (at least) two resonances, the GOR which was located from the small angle spectra 3° – 4° at 18.7 MeV, and a higher energy resonance (21.3 MeV). The GOR cross sections are well described in the whole angular range (Fig. 6), its location is in good agreement with results from (e, e') (Ref. 5) and 800 MeV (p, p') (Ref. 2) scattering. Details of this excitation are presented elsewhere.¹⁷ The data for the 21.3 MeV resonance are consistent with a $L=1$ structure: in the 6° region the relative yield is large whereas in the 3° – 4° region this resonance has not been observed. At larger angles the $L=1$ prediction is generally too low (dashed line in Fig. 6). There are two possibilities to account for the larger experimental yields. One is the assumption of additional multipole strength in this region. $L=5$ excitation which has been predicted theoretically²² would yield an improved fit to the data (Table I, fit 2). The solid line for the 21.3 MeV resonance in Fig. 6 is obtained by assuming in addition to the $L=1$ yields a $L=5$ component of 5% EWSR strength. The other possibility is a stronger $L=1$ excitation. As already discussed for the monopole excitation, surface effects can lead to larger absolute cross sections for compression modes. Here, it should be noted that the different isoscalar dipole form factor of Ref. 34 yields absolute cross sections larger by a factor of about 1.7. In this approach a transition operator of the form $r^3 Y_1$ has been assumed in a potential approach.

Recently, our evidence for a $1^- T=0$ excitation at 21.3 MeV has been confirmed in 200 MeV p scattering.⁴ To test if our transition density (1) yields an adequate description of the squeezing mode we performed DWBA calculations for (p, p') similar to those discussed above. The same nucleon-nucleon interaction of Gaussian form was used but with a reduced volume integral of 180 MeV fm^3 . This is obtained from the optical potential for 200 MeV proton scattering (see Ref. 4) which was used to describe the distorted waves in coming and outgoing channels. An excellent description of the data of Ref. 4 is obtained (Fig. 12). The small angle cross sections are mainly due to isovector quadrupole excitation (dashed line in Fig. 12) excited by the Coulomb force. Our fit is of the same quality as the microscopic distorted-wave impulse approximation (DWIA) calculations presented in Ref. 4. From our results we cannot support the conclusions of Ref. 4 that a macroscopic DWBA calculation is inferior to a microscopic DWIA calculation at 200 MeV (p, p') . Certainly it is necessary to use a folding approach, but ρ_{TR} can be taken from microscopic as well as macroscopic models. Our

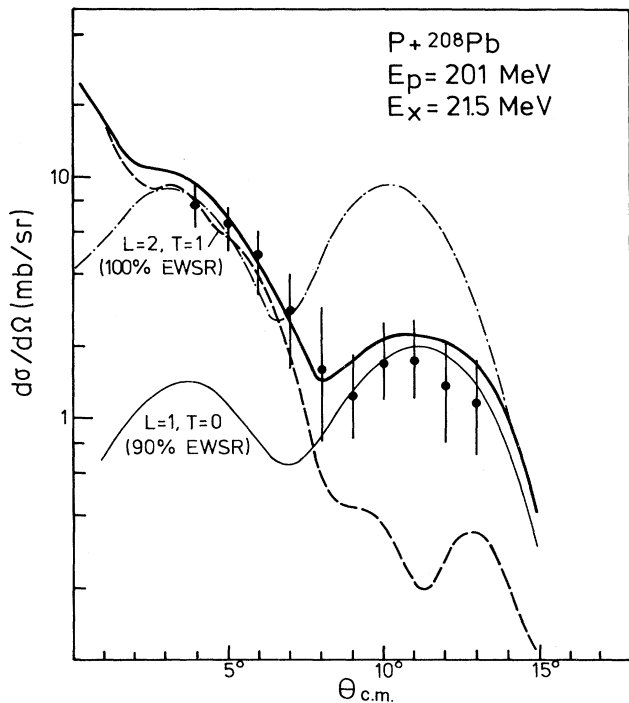


FIG. 12. Comparison of 201 MeV (p, p') data of Ref. 4 with calculated cross sections consistent with our results for the 21.3 MeV resonance (thick solid line) assuming isocalar dipole excitation (thin solid line) using the transition density in Eq. (1) and Coulomb excitation of the isovector quadrupole resonance (dashed line) which is at about the same excitation energy. The dot-dashed line is obtained using the isocalar dipole form factor of Ref. 34.

transition density (1) for the squeezing mode is not much different from that obtained from RPA calculations.³⁵ It should be noted that the rather different approach of Ref. 34 (dot-dashed line in Fig. 12) does not give a reasonable account of the experimental data on (p, p'). This is not so much due to a deficiency of the transition density [effects up to (30–50)% are expected] but mainly due to the fact that exact folding was not applied.

IV. CONCLUDING REMARKS

The present study of small angle α scattering from ^{208}Pb has revealed a rather complex giant resonance structure in ^{208}Pb which could only be disentangled by the possibility to take small angle scattering data. The very for-

ward angle data given information on the isocalar strength of low multiplicities $L=0$ and 2 whereas higher multiplicities could be detected rather unambiguously in the angular region 5° – 8° . From our experimental results it was possible to determine the distributions of $2\hbar\omega$ $L=2$, 4, and 6 excitations and study in more detail the odd parity high lying resonances: The location and width of the GOR could be determined rather accurately in the angular region 3° – 4° , also the existence of an isocalar dipole resonance (“squeezing mode”) is confirmed by our data. From the possibility to study the compression modes at high α energy under extreme conditions— isocalar dipole mode at 2° and monopole mode at 0° —it may be possible to extract detailed information on the transition densities of these important modes of excitation.

In addition to the new information on multipole strength distributions two actual problems could be solved: the unusually large α scattering cross sections for the GMR excitation and the isocalar $L=2$ strength in the GQR region. By the present finding of a large $L=4$ concentration at 12.5 MeV the monopole cross section was lowered considerably (up to 40% at certain angles). A consistent description of small and larger angle data is obtained assuming a monopole cross section compatible with microscopic and macroscopic models.^{10,14,15}

Concerning the isocalar $L=2$ excitation, we find $(60 \pm 10)\%$ EWSR strength in the 10.9 MeV region, the total $L=2$ strength in the $2\hbar\omega$ excitation region amounts to $(70 \pm 20)\%$ of the EWSR limit. This result is in agreement with theoretical models^{10,22,31} and confirms other hadron and higher energy electron scattering results. There may be two reasons why in lower energy electron scattering the isocalar $E2$ strength could be underestimated so much. First, the dynamics at lower energy (e, e') is not very favorable to excite the GQR (discussed in Sec. I) which gives rise to problems in the extraction of the large giant resonance background. On the other hand, there could be also an interesting structure aspect. Different from α scattering which is almost a purely isocalar probe²³ in (e, e') isocalar and isovector structures are excited. Owing to isospin mixing there could be appreciable differences between isocalar and electromagnetic excitation even in the region of the strong isocalar resonances. Recent microscopic calculations³¹ have indeed shown differences between these excitation mechanisms with a much broader distribution of electromagnetic $E2$ strength. Thus the detection of real differences between hadron and electron scattering may open up the possibility of studying isospin mixing and the resulting differences in proton and neutron strength at high excitation energies.

*On leave from Institute of Experimental Physics, University of Warsaw, Warsaw, Poland.

†On leave from Institute for Nuclear Research, Warsaw, Poland.

¹H. P. Morsch, M. Rogge, P. Turek, and C. Mayer-Böricke, Phys. Rev. Lett. **45**, 337 (1980).

²T. A. Carey, W. D. Cornelius, N. J. DiGiacomo, J. M. Moss, G. S. Adams, J. B. McClelland, G. Pauletta, C. Whitten, M.

Gazzaly, N. Hintz, and C. Glashauser, Phys. Rev. Lett. **45**, 239 (1980).

³T. Yamagata, S. Kishimoto, K. Yuasa, K. Iwamoto, B. Saeki, M. Tanaka, T. Fukuda, I. Mirua, M. Inoue, and H. Ogata, Phys. Rev. C **23**, 937 (1981).

⁴C. Djalali, N. Marty, M. Morlet and A. Willis, Nucl. Phys. **A380**, 42 (1982).

⁵M. Nagao and Y. Torizuka, Phys. Rev. Lett. **30**, 1068 (1973);

- M. Sasao and Y. Torizuka, Phys. Rev. C **15**, 217 (1977).
- ⁶D. H. Youngblood, J. M. Moss, C. R. Rozsa, J. D. Bronson, A. D. Bacher, and D. R. Brown, Phys. Rev. C **13**, 994 (1976).
- ⁷M. N. Harakeh, K. v. d. Borg, T. Ishimatsu, H. P. Morsch, A. v. d. Woude, and F. E. Bertrand, Phys. Rev. Lett. **38**, 676 (1977).
- ⁸H. P. Morsch, C. Sükösd, M. Rogge, P. Turek, and C. Mayer-Böricke, Phys. Rev. C **22**, 489 (1980).
- ⁹G. Kühner, D. Meuer, S. Müller, A. Richter, E. Spamer, O. Titze, and W. Knüpfer, Phys. Lett. **104B**, 189 (1981).
- ¹⁰For a summary of theoretical work, see J. Speth and J. Wambach, Nucl. Phys. **A347**, 389 (1980).
- ¹¹F. R. Buskirk, H.-D. Gräf, R. Pitthan, H. Theissen, O. Titze, and Th. Walcher, Phys. Lett. **42B**, 194 (1972); A. Schwierczinski, R. Frey, A. Richter, E. Spamer, H. Theissen, O. Titze, Th. Walcher, S. Krewald, and R. Rosenfelder, Phys. Rev. Lett. **35**, 1244 (1975).
- ¹²H. P. Morsch, P. Decowski, and W. Benenson, Phys. Rev. Lett. **37**, 263 (1976); Nucl. Phys. **A297**, 317 (1978).
- ¹³F. E. Bertrand, G. R. Satchler, D. J. Horen, J. R. Wu, A. D. Bacher, G. T. Emery, W. P. Jones, D. W. Miller, and A. v. d. Woude, Phys. Rev. C **22**, 1832 (1980).
- ¹⁴J. P. Blaizot and B. Grammaticos, Nucl. Phys. **A355**, 115 (1981).
- ¹⁵G. Eckart and G. Holzwarth, Phys. Lett. **87B**, 147 (1979).
- ¹⁶R. de Haro, J. Wambach, S. Krewald, and J. Speth, in Proceedings of the International Conference on Nuclear Structure, Amsterdam, 1982, edited by A. v. d. Woude and B. J. Verhaar, p. 103.
- ¹⁷H. P. Morsch, M. Rogge, P. Turek, P. Decowski, L. Zemło, C. Mayer-Böricke, S. A. Martin, G. P. A. Berg, I. Katayama, J. Meissburger, J. G. M. Römer, R. Reich, P. Wucherer, and W. Brätigam, Phys. Lett. **119B**, 311 (1982).
- ¹⁸M. Köhler, K. D. Müller, H. Stoff, M. Teske, G. P. A. Berg, A. Hardt, S. Martin, C. Mayer-Böricke, J. Meissburger, Nucl. Instrum. Methods **175**, 357 (1980).
- ¹⁹H. P. Morsch, M. Rogge, P. Turek, C. Mayer-Böricke, and P. Decowski, Phys. Rev. C **25**, 2939 (1982).
- ²⁰H. C. Chiang and J. Hüfner, Nucl. Phys. **A349**, 466 (1980).
- ²¹G. F. Bertsch and O. Scholten, Phys. Rev. C **25**, 804 (1982).
- ²²R. de Haro, S. Krewald, and J. Speth, Nucl. Phys. **A388**, 265 (1982).
- ²³P. Decowski and H. P. Morsch, Nucl. Phys. **A377**, 261 (1982).
- ²⁴T. Yamagata, S. Kishimoto, K. Yuasa, B. Saeki, K. Iwamoto, M. Tanaka, T. Fukuda, I. Miura, M. Inoue, and H. Ogata, Nucl. Phys. **A381**, 277 (1982).
- ²⁵H. P. Morsch and P. Decowski, Phys. Lett. **95B**, 160 (1980).
- ²⁶P. Decowski, H. P. Morsch, and W. Benenson, Phys. Lett. **101B**, 147 (1981).
- ²⁷Owing to the discovery of the giant octupole resonance which has a large $L = 3$ sum rule strength fit 2 in Table VI of Ref. 8 can be excluded.
- ²⁸H. Steuer, W. Eyrich, A. Hofmann, H. Ortner, U. Scheib, R. Stamminger, D. Steuer, and H. Rebel, Phys. Rev. Lett. **47**, 1702 (1981).
- ²⁹R. Pitthan and F. R. Buskirk, Phys. Rev. C **16**, 983 (1977); see also R. Pitthan, H. Hass, D. H. Meyer, F. R. Buskirk, and J. N. Dyer, *ibid.* **19**, 1251 (1979).
- ³⁰R. D. Starr, P. Axel and L. S. Cardman, Phys. Rev. C **25**, 780 (1982); Z. W. Bell, L. S. Cardman, and P. Axel, *ibid.* **25**, 791 (1982).
- ³¹J. Wambach (private communication); B. Schwesinger and J. Wambach, Stony Brook Report, 1982.
- ³²P. Decowski, H. P. Morsch, and C. Sükösd (unpublished).
- ³³M. Brack and W. Stocker, Nucl. Phys. **A388**, 230 (1982).
- ³⁴M. N. Harakeh and A. E. L. Dieperink, Phys. Rev. C **23**, 2329 (1981).
- ³⁵J. Wambach, V. Klemt, and J. Speth, Phys. Lett. **77B**, 245 (1978); N. van Giai and H. Sagawa, Nucl. Phys. **A371**, 1 (1981).